Seasonal soil moisture changes under mat foundations in Nicosia marl

G. Lazarou[1], D. Loukidis[1], M. Bardanis[2]

[1] **Department of Civil & Environmental Engineering, University of Cyprus, Nicosia, Cyprus**
[2] **Edafos Engineering Consultants S.A., Athens, Greece**

1 Introduction

Expansive soils cause damages of various degrees to civil engineering structures, costing tens of billion dollars annually worldwide. These soils can be found in wide areas of Cyprus, like the Mesaoria basin between the Troodos and Kerynia mountain ranges and along the southern coastline. Cyprus' climate is characterized by large seasonal contrasts (rainy winters and dry/hot summers), aggravating the adverse effects of soil swelling/shrinkage on civil engineering structures.

This paper presents the results of an investigation of the phenomenon of moisture migration under a foundation slab (mat) in Nicosia marl, the predominant expansive soil of Cyprus. First, the hydraulic and water retention characteristics of the marl are determined based on laboratory tests and a field wetting experiment. Subsequently, unsaturated flow parametric finite element analyses were performed for the numerical investigation of moisture migration under an impermeable mat with climatic input consistent with the Nicosia area, in order to investigate the influence of the mat thickness, soil permeability, and the presence or absence of a shallow water table on the moisture fluctuations under the mat.

2 Laboratory experiments

2.1 Trial Pit Sampling and Borehole Drilling

The Nicosia marl is a Pliocene stiff clay belonging to the Nicosia geological formation and has a thickness that reaches several hundred meters (Consatantinou et al., 2002). Samples of Nicosia marl were collected from the site of the new University of Cyprus (UCY) campus located in Mesaoria basin. The soil samples were collected from a trial pit 1.5m deep excavated in July 2015 (block samples) and a borehole drilled in May 2015 (U100 tube samples). The trial pit samples were protected by wrapping them in cling film and plastic bags, while the borehole samples by covering the ends of the tube samplers with molten paraffin wax.

Fig. 1 presents the soil stratigraphy in the area of the study. The Nicosia marl consists of two parts; the brown (also described as khaki) marl and the grey marl. The first can be found in the upper part of the Nicosia geological formation and is stiffer and more calcareous than the grey marl found at greater depths. The brown marl is also more expansive because, despite being more calcareous, has a significant amount of montmorillonite, which in certain parts of Nicosia reaches 26% (Atalar, 2011), than the grey marl. The brown marl horizon at the study site is itself non-uniform, with the upper layer having calcium carbonate ($CaCO_3$) content of the order of 40%-50% and low clay content, while deeper brown marl layers are more clayey. As a result, according to the "South African chart" (Van der Merwe, 1975), the upper, hard brown marl is characterized as medium to highly expansive, while the underlaying softer brown marl is characterized as very highly expansive (Loukidis et al., 2016). The water table at the study site is relatively shallow (at 7m-7.5m depth at the location of the trial pit) due to the presence of two small reservoir dams in the region.

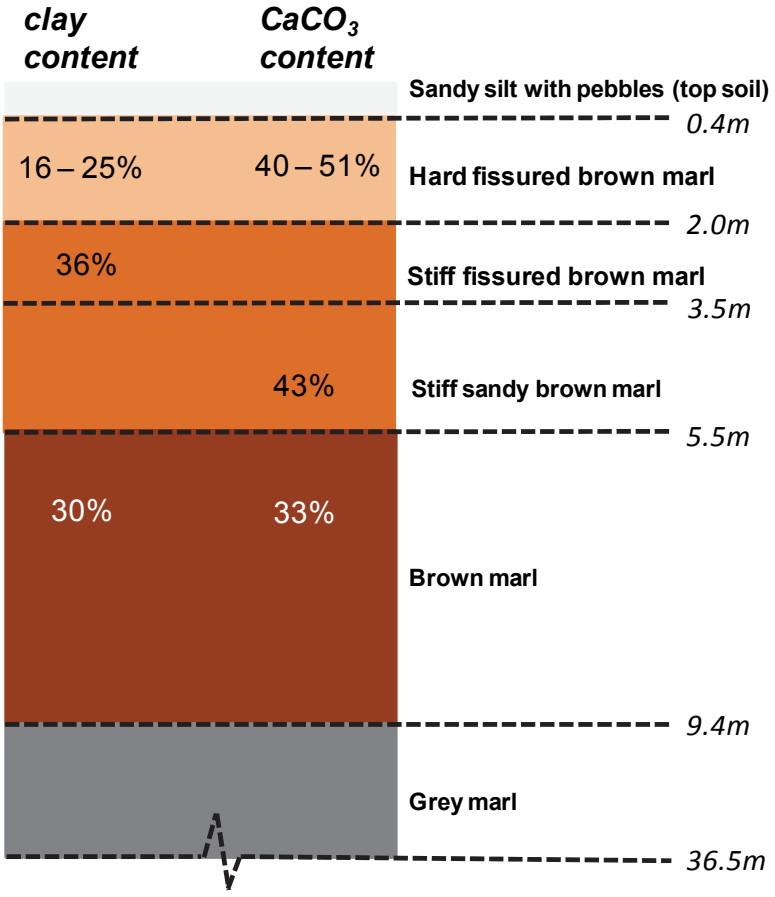

Fig. 1: Simplified soil stratigraphy at the study area

2.2 Soil –Water Characteristic Curve (SWCC)

The SWCC was determined for the hard brown marl (Fig. 2) in terms of total suction using a chilled mirror hygrometer (WP4, Decagon Inc.). The samples

transferred to the laboratory were left sealed for a few days in order to reach equilibrium regarding moisture, before any suction measurement at natural state. To establish the drying and wetting portions of the SWCC, some samples were left to air-dry while others were wetted, in both cases gradually from their natural water content. The soil volume measurements were done by immersing the samples in molten paraffin wax, which combined with mass and water content of the specimens, permit the estimation of the void ratio and the degree of saturation S_r. As shown in Fig. 2, when the degree of saturation reaches 80%, the corresponding total suction reaches about 600kPa and, when the soil is almost dry (residual saturation equals to 10%), it increases up to 150MPa. At natural water content 10%≤w≤14% (39%≤S_r≤57%) total suction s was 5700kPa≤s ≤8750kPa. The highest suction at natural state was measured in an undisturbed sample from tube sampler, a fact indicating that the block samples were only marginally affected by drying during transportation to the laboratory.

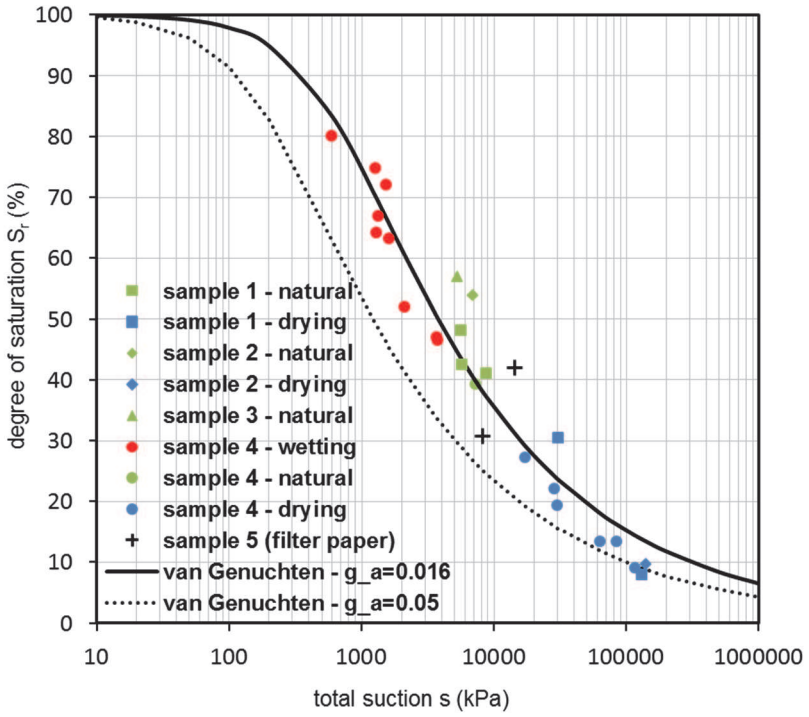

Fig. 2: Soil-water characteristic curve of the hard brown marl.

The SWCC in Fig. 2 is in terms of the total suction. Field matric suction sensors installed in the trial pit measured in September 2015 a matric suction around 750kPa, much lower than total suction measured in the laboratory, while, in summer 2016, the matric suction exceeded 1000kPa. This large difference between total and matric suctions suggest that the osmotic suction exceeds 1MPa. To certify the presence of high osmotic suction, contact (matric suction) and non-contact (total suction) filter paper tests (ASTM D5298-10) were conducted on a recompacted specimen and an undisturbed (sawed in two parts) specimen. Total

suction for recompacted and intact specimens was 8.2MPa and 14.3MPa and matric suction 4.3MPa and 9.5MPa, respectively. These values indicate that the osmotic suction is 3.9MPa to 4.7MPa for water content in the 10%-12% range. The presence of high salt concentration was later verified by soil chemical analysis, which yielded electrical conductivity of 6mS/cm, salinity of 0.3g/100g and sodium cations Na^{++} meq/100g =3.2.

Fig. 2 presents also SWCC fitting using the Van Genuchten (1980):

$$S_{\mathrm{r}}(s) = S_{\mathrm{r,res}} + \left(1 - S_{\mathrm{r,res}}\right)\left[1 + \left(g_a \left|\frac{s}{\gamma_{\mathrm{w}}}\right|\right)^{g_{\mathrm{n}}}\right]^{g_{\mathrm{c}}} \quad (1)$$

where S_{r} is the degree of saturation, s is the soil suction and γ_w is the water unit weight, $S_{\mathrm{r,res}}$ is the residual degree of saturation and g_{a}, g_{n} and g_{c} are fitting parameters. The parameter g_c is set equal $(1\text{-}g_{\mathrm{n}})/g_{\mathrm{n}}$, reducing eq. (1) to a three-parameter expression (Mualem, 1976). The optimal values for the fitting parameters are g_{a}=0.016, g_{n}=1.37 and $S_{\mathrm{r,res}}$=0. Fig. 2 also plots the curve (dashed line) corresponding to g_{a}=0.05, which would better represent the SWCC in terms of matric suction (750kPa measured by the field sensors at S_{r}=55%). Both g_{a} values were considered in the trial and error back-calculation simulations of the field wetting experiment because it is uncertain to what degree the unsaturated groundwater flow depends on the matric suction or the total suction, and given the fact that the FE software used considers only a single flow mechanism.

3 Field Wetting Experiment

The sampling trial pit was also used for installing is-situ pairs of GS3 volumetric water content sensors and MPS-6 matric suction sensors (by Decagon Devices Inc.). The field sensors were embedded in the pit walls at two difference depths (0.75m and 1.5m) and connected to an automatic Em50 data logger for continuous data recording. Great attention was paid when backfilling the pit in order to use almost the entire quantity of the excavated material, targeting in having a final density similar to that of the undisturbed marl.

The sensors were used in a field wetting experiment (Hillel et al., 1972; Toll et al., 2012) performed in Fall 2015 in order to determine the in-situ hydraulic characteristics of the Nicosia marl. The in-situ hydraulic conductivity is expected to be greater than the one measured in the laboratory on intact samples (Benson & Gibbs, 1997) due to desiccation cracks and structural discontinuities. The wetting of the ground was achieved through a circular pond of 1m diameter with its center at the same vertical line with the sensors. The wetting experiment consisted of wetting (filling a pond of 0.5m radius with water of known volume) and non-wetting (water absorption) phases. Fig. 3a shows the time history of the degree of

saturation at 0.75m and 1.5m depth, based on the recordings of the GS3 sensors. Full saturation of the soil at 0.75m depth was achieved on 6/10/2015 (at about 6000min), whereas the full saturation front reached 1.5m depth on 17/10/2015 (at about 21600min).

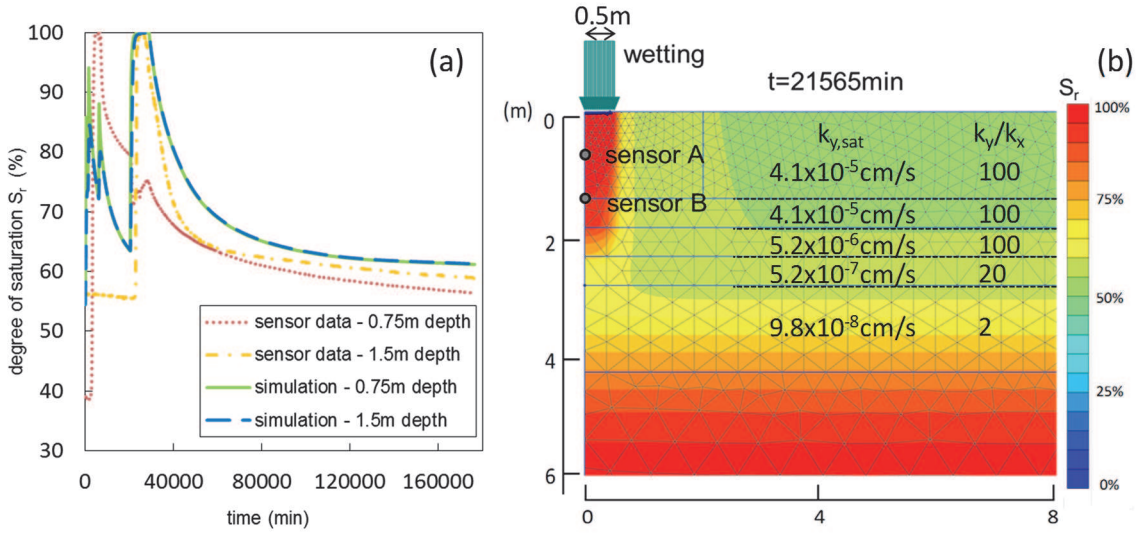

Fig. 3: Field wetting experiment: a) degree of saturation time histories and b) contours from FE simulation.

After having the required data from the wetting experiment, a finite element (FE) program (Plaxis) was used to simulate it in order to back-calculate the in-situ hydraulic properties of the Nicosia marl (Fig. 3b). Trial and error simulations were performed to match the time history of the degree of saturation S_r at both sensor depths by changing: 1) the coefficient of hydraulic conductivity in the y-direction under full saturation conditions $k_{y,sat}$, 2) the ratio of vertical to horizontal hydraulic conductivity $k_{y,sat}/k_{x,sat}$ and 3) the dependence of the unsaturated hydraulic conductivity on the soil suction (eq. 2). The hydraulic conductivity measured in the laboratory using flexible wall permeameter was taken as the basis in the trial and error analyses, in the sense that the apparent in-situ $k_{y,sat}$ is not allowed to be smaller than that of the intact samples.

The dependence of the unsaturated hydraulic conductivity on the soil suction (through S_r) in the FE program is given by (Galavi, 2010):

$$k(s) = k_{sat}\left(\frac{S_r(s)-S_{r,res}}{1-S_{r,res}}\right)^{g_l}\left[1-\left(1-\left(\frac{S_r(s)-S_{r,res}}{1-S_{r,res}}\right)^{-\frac{1}{g_c}}\right)^{-g_c}\right]^2 \qquad (2)$$

where k_{sat} is the hydraulic conductivity of the soil when fully saturated and g_l is a model parameter. In the FE simulations, it was assumed that the SWCC of the hard brown marl applies to the whole modeled soil profile.

A large number of of trial-and-error simulations were performed until the best possible convergence was achieved between the measured time history of S_r and the one yielded by FEA, focusing mainly on the progressive desaturation after full saturation has reached sensor B at 1.5m depth (t>23000min). The optimal permeability values are shown in Fig. 3b, while g_a=0.016 and g_l=-5 are set throughout the profile. Discrepancies between the observed and predicted time histories can be attributed to: 1) the assumption that the moisture migration phenomenon is governed exclusively by the flow of water, ignoring the effects of the air permeability and the hydration of active clay minerals of the marl and 2) neglecting the hysteresis in the SWCC. The back-calculated permeability for the upper 2m of the profile (the desiccated crust) is much larger (two orders of magnitude) than the one measured in the laboratory (2.60×10^{-7} cm/s), a fact that is consistent with the findings of Ankeny et al. (1991) and Tsaparas and Toll (2002).

4 Simulations of Moisture Migration under a Mat

Having established the field permeability of the marl at the study site, parametric finite element analyses (FEA) of moisture migration under a circular mat foundation (2D axisymmetric problem) were performed for the climatic input of the period May 2014 - September 2015, which includes an above rainy winter and two very dry summers. The radius of the mat was 10m, while the width and the thickness of the soil domain were 40m and 8m respectively. The lateral boundaries were set to be closed (no flow) and the lower boundary was left open for water to drain or infiltrate depending on the level of the water table. At the free ground surface, rainfall (positive infiltration) and evapotranspiration (negative infiltration) were applied during rainy and non-rainy days respectively. The daily rainfall data comes from the Cyprus Department of Meteorology while the applied evapotranspiration was derived based on pan evaporation data according to Metochis (1977) scaled down to match the net yearly water input, a condition that is consistent with arid climates. It should be noted that the parametric analyses were flow only simulations and any effects of soil swelling/shrinkage and mechanical interaction between mat and soil are ignored.

The parametric analyses examined the effects of the mat thickness d, the marl hydraulic conductivity and the presence of a shallow water table (7m depth). The examined analysis output is in the form of the spatial and temporal variation of S_r and suction s. Fig. 4 presents examples of contours of S_r for selected months for a 0.5m thick mat on marl having g_a=0.016, g_l=-5 and the permeability inferred by

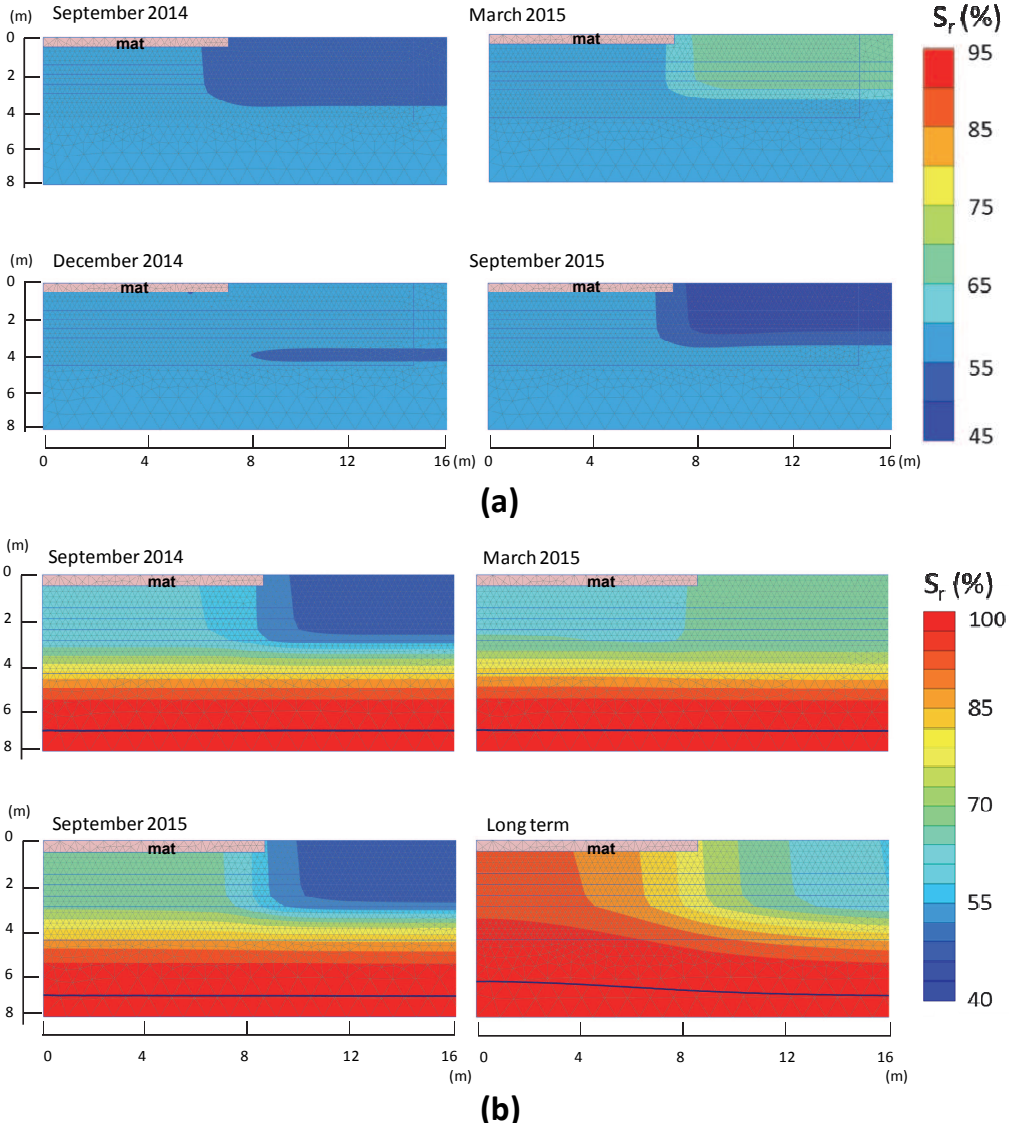

Fig. 4: Contours of degree of saturation for selected months in the vicinity of a mat: a) in the absence and b) in the presence of a shallow water table.

the field wetting experiment, in the absence and in the presence of a shallow water table. Moreover, Fig. 5 presents the distribution of S_r and s at the mat-soil interface from the same analyses, for end of March 2015 (end of rainy season) and end of September 2015 (end of dry season). The S_r for shallow layers not covered by the mat ranges from 45% in September to 67% in March. During summer months (June to September), the S_r in a 3m wide edge region of the mat decreases, leading to an increase in suction of the order of 1MPa (Fig. 5), as moisture migrates away from the mat center, while the opposite happens during winter months (December to March). Nonetheless, in the presence of the shallow water table (Figs. 4b, 5b), there is a significant ascent of moisture in the long-term (40yrs period) from the water table towards the slab central region, where S_r reaches 93%. This is because the slab acts as an impermeable boundary blocking the natural escape of moisture from the water table to the atmosphere caused by evapotranspiration. Hence, the presence of a shallow water table in a practical

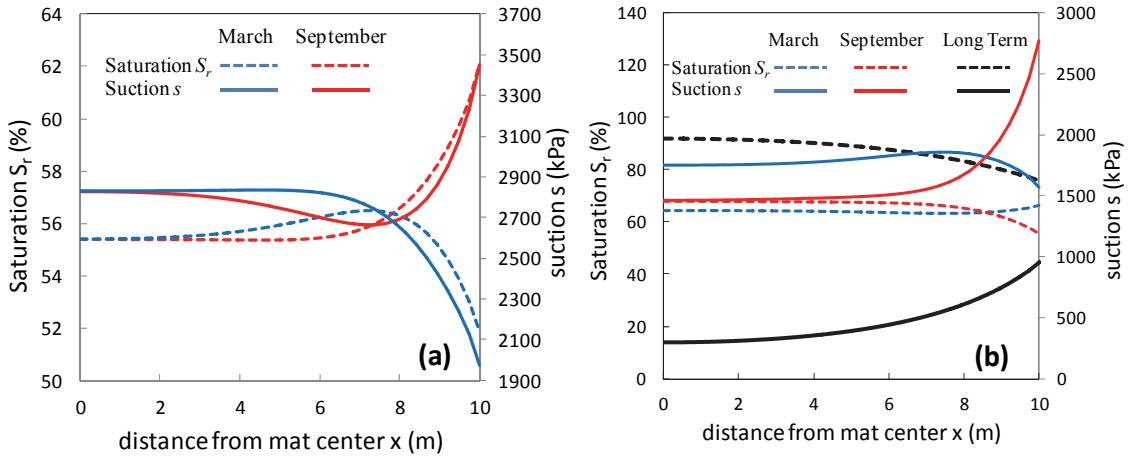

Fig. 5: Degree of saturation distributions at the soil-mat interface: a) in the absence and b) in the presence of a shallow water table.

situation will lead to severe soil swelling under the mat central region, giving rise to the damaging phenomenon often called "center heave".

Fig. 6 presents results from analyses with different mat thickness value in the absence of shallow water table. It is observed that the S_r variation underneath the slab is practically the same for depth of mat-soil interface in the range of 0.5m to 2m. This is because i) the ground down to 2m depth belongs to a desiccated crust where suction s is almost constant and large $k_{y,sat}$ values favor the moisture penetration to this depth and ii) the decrease in $k_{y,sat}$ in greater depths hampers further moisture migration in the vertical direction, forcing more migration in the horizontal direction (and thus under the slab).

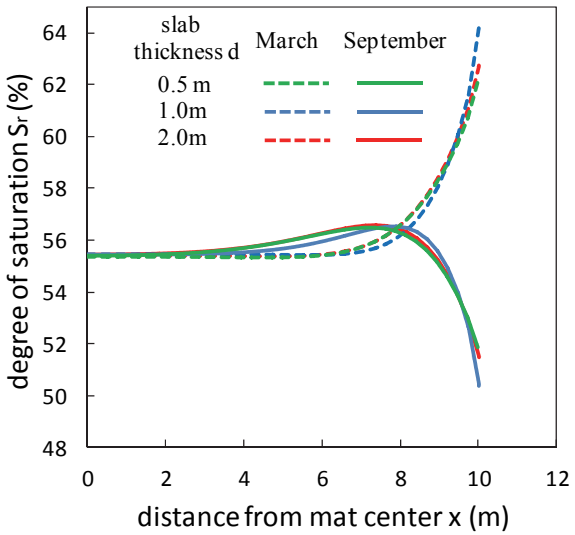

Fig. 6: Distribution of S_r underneath mat for various values of mat thickness.

Fig. 7 shows results from analyses with 3 different hydraulic conductivity k_{sat} profiles (with profile A being the same as the back-calculated one). This figure indicates that forcing $k_{y,sat}$ to be equal to $k_{x,sat}$ (profile C) leads to more extended

and intense moisture variation under the mat. Moreover, a tenfold decrease in both $k_{y,sat}$ and $k_{x,sat}$ (profile B) results in a much narrower (1.5m-2m) region of moisture variation at the mat edge.

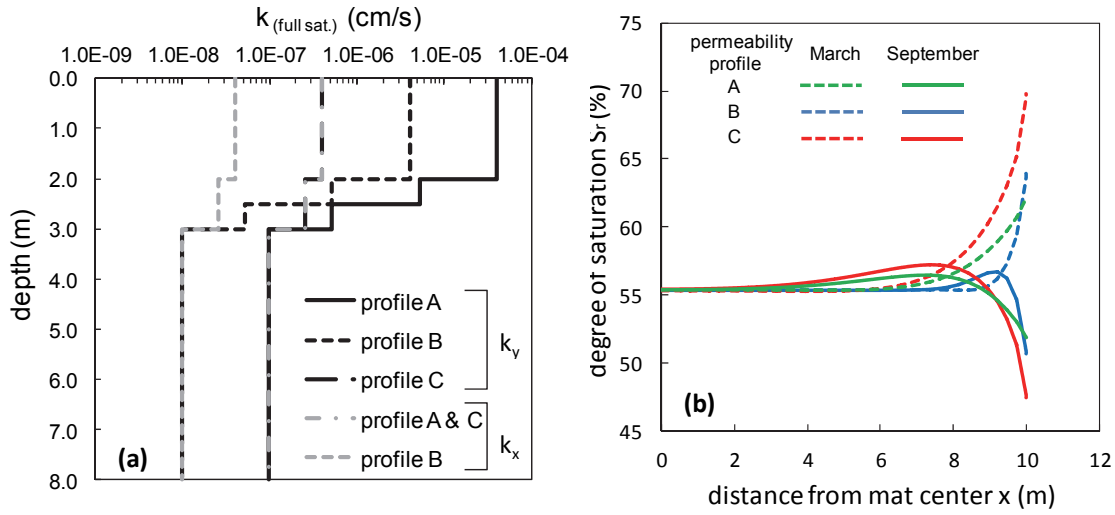

Fig. 7: Distribution of S_r underneath mat for various permeability soil profiles.

5 Conclusions

From the results of the present study the following conclusions may be drawn:

- The full saturation hydraulic conductivity of the desiccated crust has to be two orders of magnitude larger than the one measured in the laboratory in intact specimens in order for the simulations to match field observations.
- The seasonal fluctuations of S_r are localized at the edge region of the mat foundation, the width of which depends on the soil hydraulic characteristics.
- The mat acts as an impermeable boundary that blocks natural evapotranspiration, leading to a long-term rise of moisture from a shallow water table towards the mat central part.
- In the absence of a shallow water table, the variation of S_r beneath the slab is only slightly affected by the depth of the mat-soil interface.

6 Literature

Ankeny, M. D., Ahmed, M., Kaspar, T. C. & Horton, R. (1991). Simple field method for determining unsaturated hydraulic conductivity. Soil Science Society of America Journal, 55(2), 467-470.

ASTM (2010). Designation: D5298-10. Standard Test Method for Measurement of Soil Potential (Suction) Using Filter Paper.

Atalar, C. (2011). A review of the origin and properties of the soils of Nicosia, Cyprus. International Journal of Geotechnical Engineering, 5(1), 79-86.

Benson, C. & Gribbs, M. (1997). Measuring unsaturated hydraulic conductivity in the laboratory and the field. Geotechnical Special Publication, 113-168.

Constantinou, G., Panagides I., Xenophontos, K., Afrodisis, S., Michaelides, P. & Kramvis, S. (2002). The geology of Cyprus (Bulletin No. 10, Cyprus Geological Survey).

Galavi, V. (2010). Groundwater flow, fully coupled flow deformation and undrained analyses in PLAXIS 2D and 3D (p. 290). Internal Report, Delft, Netherlands: PLAXIS bv Research Department.

Hillel, D., Krentos, V. D. & Stylianou, Y. (1972). Procedure and test of an internal drainage method for measuring soil hydraulic characteristics in situ. Soil Science, 114(5), 395-400.

Loukidis, D., Bardanis, M. & Lazarou, G. (2016). "Classification, soil-water characteristic curve and swelling/collapse behaviour of the Nicosia marl, Cyprus." Proceedings of the 3rd European Conference on Unsaturated Soils E-UNSAT 2016, Paris, France.

Metochis, C. (1977). Potential Evapotranspiration of Lucerne, (Bulletin No. 21, Agricultural Research Institute, Ministry of Agricultural and Natural Resources).

Mualem, Y. (1976). A new model for predicting the hydraulic conductivity of unsaturated porous media. Water resources research, 12(3), 513-522.

Toll, D. G., Mendes, J., Gallipoli, D., Glendinning, S. & Hughes, P. N. (2012). Investigating the impacts of climate change on slopes: field measurements. Geological Society, London, Engineering Geology Special Publications, 26(1), 151-161.

Tsaparas, I. & Toll, D. G. (2002). Numerical analysis of infiltration into unsaturated residual soil slopes. In Proc. 3rd International Conference on Unsaturated Soils, Recife, Brazil, Lisse: Swets & Zeitlinger (Vol. 2, pp. 755-762).

Van Genuchten, M. T. (1980). A closed-form equation for predicting the hydraulic conductivity of unsaturated soils. Soil Science Society of America Journal, 44(5), 892-898.

Van der Merwe, D. H. (1975). Plasticity index and percentage clay fraction of soils. Proceedings of the 4th Regional Conference in Africa on Soil Mechanics and Foundation Engineering, Vol. 2, 166-167.